

Real-Time Backstepping Control for Fuel Cell Vehicle using Supercapacitors

C. Dépature, W. Lhomme, *Member, IEEE*, P. Sicard,
A. Bouscayrol, *Member, IEEE*, L. Boulon, *Senior Member, IEEE*

Abstract — A key issue of real-time applications is ensuring the operation by taking into account the stability constraints. For multi-source vehicles stability is impacted by the multi-source interactions. Backstepping control ensures stable control for most classes of nonlinear systems. Nevertheless, no Backstepping control in real-time has been yet proposed for multi-source vehicles. The objective of this paper is to apply the Backstepping control to a multi-source vehicle with fuel cell and supercapacitors for real-time implementation. A distribution criterion is used to allocate energy between sources. Experimental results demonstrate that the developed Backstepping control can be implemented in real-time conditions. The supercapacitors can thus help the fuel cell to meet the requirements of the load with a guarantee of system stability.

Index Terms—Keywords: *Backstepping control, Electric vehicle, Fuel cell, Multi-source, Real-time, Ultracapacitor*

NOMENCLATURE

Variables		Subscripts	
C	Capacitance [F]	1,2,3	Loop index number
c	Positive constant [-]	bus	DC bus
G	Transfer function [-]	ed	Electric drive
i	Electric current [A]	fc	Fuel cell
L	Inductance [H]	ch	Chopper
P	Power [W]	s	Electrical source
r	Resistance [Ω]	sc	Supercapacitor
u	Voltage [V]	ts	Traction subsystem
V	Lyapunov control function [-]		
α	Chopper duty cycle [-]		
η	Efficiency [%]		
θ	Unknown parameter [-]		
Γ	Adaptation gain [-]		

Copyright (c) 2015 IEEE. Personal use of this material is permitted. However, permission to use this material for any other purposes must be obtained from the IEEE by sending a request to pubs-permissions@ieee.org.

C. Dépature is with the Univ. Lille, Centrale Lille, Arts et Métiers Paris Tech, HEI, EA 2697 L2EP - Laboratoire d'Electrotechnique et d'Electronique de Puissance F-59000 Lille, France and with the GREI, Université du Québec à Trois-Rivières, Canada (e-mail: Clement.Depature@uqtr.ca).

W. Lhomme and A. Bouscayrol are with the Univ. Lille, Centrale Lille, Arts et Métiers Paris Tech, HEI, EA 2697 L2EP - Laboratoire d'Electrotechnique et d'Electronique de Puissance F-59000 Lille, France (e-mail: Walter.Lhomme@univ-lille1.fr; Alain.Bous-cayrol@univ-lille1.fr).

P. Sicard and L. Boulon are with the GREI, Université du Québec à Trois-Rivières, Canada (e-mail: Pierre.Sicard@uqtr.ca; Loic.Boulon@uqtr.ca).

I. INTRODUCTION

IN the last decade there has been a growing interest in Fuel Cell (FC) vehicles. By using hydrogen, FC vehicles are a promising solution to reduce greenhouse gases [1]. However, FC systems lead to slow dynamics with a reduced lifetime when they are subjected to fast power transients. Furthermore, the energy flow of FC systems is unidirectional, which does not allow to recover braking energy [2]. Hybridization of FC with other energy storage devices can thus improve the vehicle performances. A battery can be used as a secondary source to handle the power transients, to recover braking energy, to downsize the FC, to extend its lifetime and to reduce its cost. With its Mirai car, Toyota has chosen this technology using a Ni-MH battery pack [3]. Hybridization of a FC with SuperCapacitors (SC) as energy buffer represents another interesting solution. With their high specific power and power density as compared to battery, SC can assist a FC to meet the high power requirements [2], [4]. With its FCX, Honda has chosen this technology to supply additional power to its vehicle [5]. Henceforth industrial applications are taking advantages of both battery and SC to assist FC vehicles.

The control of FC vehicles using SC must take into account the constraints related to the strong energetic coupling among the sources. Both sources are indeed connected through a DC bus. It is necessary to control and manage the energy distribution between sources. Recently, attention has been paid to the control and energy management of FC/SC vehicles using PI controllers [6], [7], flatness control [4] and fuzzy logic controllers [8]. However, most of these propositions have been evaluated only in simulation. Furthermore, these studies do not intrinsically ensure stability, especially when saturation occurs [6]. It is well established that non-linear behaviors [9] affect the system stability. Instability can cause energy losses and potentially damage on the vehicle. To solve the stability issue, several authors have proposed to use energy-based Lyapunov control theory for the controller design [10], [11]. Energy or pseudo energy functions, called control Lyapunov functions, or *clf*, are then defined to ensure the system stability. The Lyapunov stability design technique leads indeed to stabilize Multiple Input Multiple Output (MIMO) systems. More recently, new researches consist to use an extension of Lyapunov technique with the so-called "Backstepping control". The key idea of Backstepping control is to divide the MIMO system into Single Input Single Output (SISO) subsystems to define a control scheme with cascaded loops [12], [13]. In a recent paper a Backstepping control of a FC/battery vehicle

has been proposed [14]. The authors designed two current loops, for the FC and the battery. The energetic coupling between both sources and the DC bus voltage is not considered in the control loop design. Both current loops are then controlled independently, which leads to a local stability for each control loop. The stability of the whole system is thus not guaranteed.

Coupled systems have to be divided in a clear way to develop a stabilizing control law with Backstepping control technique. Nonetheless, the choice of the division of Backstepping control relies on the expertise of the user. It was shown in [15] that EMR (Energetic Macroscopic Representation) is efficient to define a systematic control scheme while the Backstepping control design ensures stability. In [16] it was also shown that EMR can be used to define the cascaded loops of FC vehicle using SC. However, the energetic coupling between sources was managed without using the Backstepping control technique. Furthermore, the Backstepping control was designed in a global approach with a mathematical state representation. All the studies cited above were performed exclusively in simulation.

This paper deals with stable control for a fuel cell vehicle using supercapacitors with a Backstepping control technique. Prior to this paper no Backstepping control in real-time had ever been considered for multi-source vehicles. The simulation of the Backstepping control of the studied FC/SC vehicle was carried out in [16]. This paper focuses on experimental tests to verify feasibility and compare the Backstepping control performances with classical PI controllers. Based on [15] and [16], the control of the FC/SC vehicle is decomposed in a clear way to design the Backstepping control. The Backstepping control is thus applied separately to each control part. Experimental tests on a test bed are performed to assess the performances of the real-time developed Backstepping control. The remainder of the paper is organized as follows. Section II describes the studied FC/SC system and depicts its model, its EMR and the corresponding control scheme. Section III describes the Backstepping control technique. Section IV is devoted to the test bed of the system with a discussion on the experimental results.

II. CONTROL ORGANIZATION

A. Modeling

A 15 kW FC/SC vehicle is considered (Fig. 1). The Energy Storage Subsystem (ESS) is composed of the FC, the SC, their corresponding smoothing inductors and choppers and a DC bus capacitor. The FC is considered as a voltage source characterized by its static polarization curve, i.e. an experimentally validated static model [9]. A series R-C model is used to consider only the fast dynamics of the supercapacitors [17]. The equations of the ESS and vehicle model are summarized in Table 1 [16]. To deal with the Backstepping control of the coupled sources, the focus is put on the FC/SC electric parallel connection. This energetic coupling distributes the power of the FC and SC subsystems to the DC bus and to the load. The currents of the FC and SC choppers, respectively i_{fc_ch} and i_{sc_ch} , are added together to generate the source current i_s . It is

modelled by the Kirchoff's current law (5). The DC bus capacitor then sets its voltage u_{bus} on the system.

B. Energetic Macroscopic Representation

EMR is a functional description of energetic systems for control purpose [15], [18], [19]. The system is divided into basic interacting subsystems. All elements are interconnected according to the action and reaction principle using exchange variables. The product of the action and reaction variables between two elements corresponds to the instantaneous power flow. Only the integral causality is considered in EMR. This property leads to defining accumulation elements by time dependent relationships, in which outputs are integral functions of inputs. Other elements are described using relationships without time dependence. The EMR of the studied vehicle has been proposed in [16] (upper part in Fig. 2). The FC, the SC and the traction subsystem are considered as electrical sources (green oval pictograms, cf. appendix). The choppers perform mono-domain conversions (orange square pictograms). The

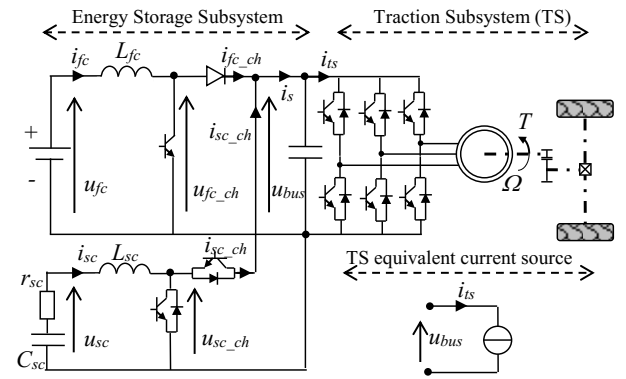


Fig. 1. Studied fuel cell/supercapacitors vehicle architecture

TABLE 1. MATHEMATICAL MODEL OF THE STUDIED FC/SC VEHICLE

DC bus	$u_{bus} = \frac{(i_s - i_{ts})}{C_{bus}s} = G_1(i_s - i_{ts})$	(1)
	with s the Laplace operator	
FC inductor	$i_{fc} = \frac{(u_{fc} - u_{fc_ch})}{(L_{fc}s + r_{fc})}$	(2)
	$= G_2(u_{fc} - u_{fc_ch})$	
SC inductor	$i_{sc} = \frac{(u_{sc} - u_{sc_ch})}{(L_{sc}s + r_{sc})}$	(3)
	$= G_3(u_{sc} - u_{sc_ch})$	
Choppers	$\begin{cases} u_{X_ch} = \alpha_{X_ch} u_{bus} \\ i_{X_ch} = \alpha_{X_ch} i_X \end{cases}$	(4)
	with $X \in [fc, sc]$	
	and $\alpha_{hX_ch} \in \{0, 1\}$	
Coupling	$i_s = i_{fc_ch} + i_{sc_ch}$	(5)
Traction Subsystem	$i_{ts} = \frac{P_m(\eta_{ed})}{u_{bus}}$	(6)

parallel connection between the FC and the SC choppers is represented by a mono-domain distribution element (overlapping squares). The smoothing inductors and the DC bus capacitor are accumulation elements (orange rectangle pictograms with diagonal line). The DC bus voltage u_{bus} , the FC current i_{fc} and SC current i_{sc} are thus the state variables of the vehicle ESS.

C. Inversion-based control scheme

From inversion rules, EMR can define an inversion-based control scheme. This kind of control is organized in two levels: local and global controls. The local control level, described by light blue parallelograms in Fig. 2, controls the components of the system. The global control level, described by a dark blue parallelogram in Fig. 2, coordinates the local control to manage the whole system. The main control objective is to impose the DC bus voltage u_{bus} to the system. Two tuning variables, the duty cycles α_{fc_ch} and α_{sc_ch} , are used to achieve this goal. The local control is then deduced by inverting the EMR from the DC bus voltage u_{bus} to the duty cycles α_{fc_ch} and α_{sc_ch} . The global control strategy block in Fig. 2, aims to manage the whole system by defining the distribution between the FC and the SC. The crossed blue parallelograms correspond to the inversion of accumulation elements using closed-loop controls. The blue parallelograms correspond to the inversion of conversion elements using open-loop control. The overlapped blue parallelograms correspond to the inversion of the energetic coupling of the sources.

Fig. 2 shows that 3 closed loop controllers are required to control the state variables i_{fc} , i_{sc} and u_{bus} . Open-loop direct inversions are needed to invert the choppers. The reference current of the coupling inversion i_{s-ref} defines two variables required by the system to control the DC bus and to manage the energy flows: the currents of the supercapacitors chopper i_{sc_ch} and of the fuel cell chopper i_{fc_ch} . This distribution results from the inversion of the energetic coupling between the choppers (5). The inversion of this coupling requires a second input to implement an energy distribution criterion, k_D in (7). k_D is provided by an energy management strategy and it links the control scheme with the strategy block. It is the key to manage the whole system.

$$\begin{cases} i_{fc_ch-ref} = k_D i_{s-ref} \\ i_{sc_ch-ref} = i_{s-ref} - i_{fc_ch-ref} \end{cases} \quad (7)$$

D. Division of the Backstepping control

Backstepping control is composed of several recursive steps that gave the method its name [12]. The key idea is to divide the MIMO system into SISO subsystems to define a control scheme with cascaded loops. The cascade closed-loop control design is defined following Lyapunov stability conditions [24]. There is no dedicated procedure to design the Backstepping control for coupled systems. The inversion-based control of EMR defines a systematic control scheme and like for the Backstepping control, the inversion-based control is composed of cascaded loops. In [16] it was shown that EMR can be used to define directly the cascaded loops of Backstepping control. Nevertheless, the energetic coupling has not been

taken into account. Herein, the inversion-based control scheme is used to define the procedure of Backstepping control by taking into account the energetic coupling. In this way, three SISO subsystems can be considered for the Backstepping control design (Fig. 3):

- A) DC bus voltage loop (BS1);
- B) FC current loop (BS2);
- C) SC current loop (BS3).

The Backstepping control is then applied separately to each control part. Hence the inversion-based control structure of EMR allows dividing directly the procedure of the Backstepping control design.

III. ADAPTIVE BACKSTEPPING CONTROL OF THE STUDIED FC/SC SYSTEM

A. DC bus voltage loop (BS1)

First, the DC bus capacitor is considered with its equation (1). The system parameters can change and disturbances act upon the system. It is then appropriate to consider unknown parameters for real-time application [22], [23]. Let us introduce unknown parameter θ_1 into (8) to include resistance or capacitance uncertainties of the DC bus capacitor. Adaptive Backstepping control technique is then used to take uncertainties into account.

$$\dot{i}_{bus} = \frac{1}{C_{bus}} (i_s - i_{ts}) + \theta_1 \quad (8)$$

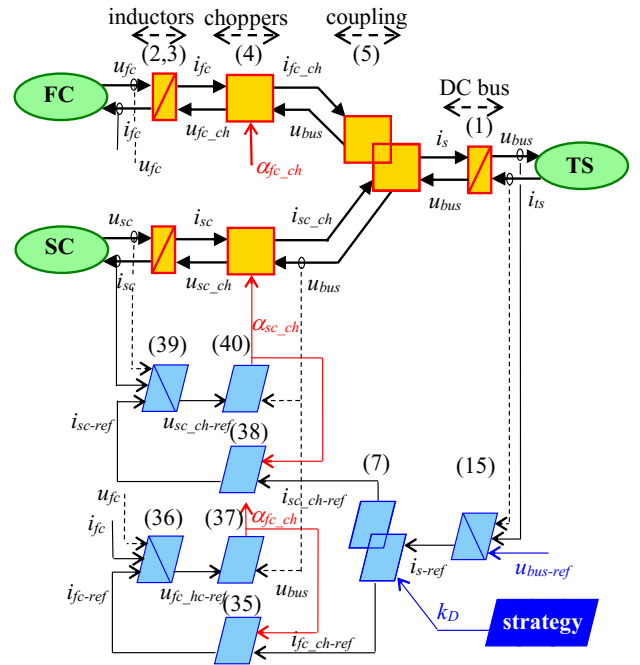


Fig. 2. EMR and control scheme of the studied vehicle

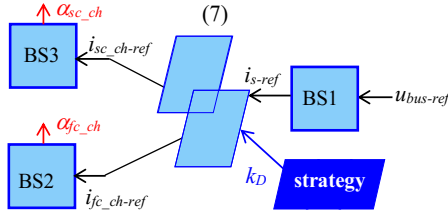


Fig. 3. Division of the Backstepping control

The objective is to deduce a local control law to control the voltage u_{bus} from the energy source current i_s . Error e_1 is defined as:

$$\begin{cases} e_1 = u_{bus-ref} - u_{bus} \\ \dot{e}_1 = \dot{u}_{bus-ref} - \frac{1}{C_{bus}}(i_s - i_{ts}) - \theta_1 \end{cases} \quad (9)$$

As θ_1 is unknown, its estimation $\hat{\theta}_1$ and estimation error $\Delta\theta_1$ are introduced as:

$$\Delta\theta_1 = \theta_1 - \hat{\theta}_1 \quad (10)$$

Here, the variations of θ_1 are assumed to be slow. A control Lyapunov function (*clf*) V_1 is proposed. It defines an image of the DC bus energy in respect with the Lyapunov-LaSalle theorems [25]:

$$\begin{cases} V_1 = \frac{1}{2} C_{bus} e_1^2 + \frac{1}{2} \Delta\theta_1 \Gamma_1^{-1} \Delta\theta_1 \\ \dot{V}_1 = C_{bus} e_1 \dot{e}_1 - \Delta\theta_1 \Gamma_1^{-1} \dot{\hat{\theta}}_1 \end{cases} \quad (11)$$

where Γ_1 is a positive constant, which will be chosen in function of the desired performances.

Using (9) and (10), introducing variable i_{s-ref} and from the assumption of slow variations of θ_1 , (11) results into

$$\begin{aligned} \dot{V}_1 = & e_1 (C_{bus} \dot{u}_{bus-ref} - (\dot{i}_{s-ref} - \dot{i}_{ts}) + C_{bus} \dot{\hat{\theta}}_1) + e_1 (\dot{i}_{s-ref} - \dot{i}_s) \\ & - C_{bus} e_1 \Delta\theta_1 - \Delta\theta_1 \Gamma_1^{-1} \dot{\hat{\theta}}_1 \end{aligned} \quad (12)$$

A term $c_1 e_1$, with $c_1 \geq 0$, is introduced to impose the Lyapunov stability condition $\dot{V}_1 \leq 0$:

$$\dot{V}_1 = -c_1 e_1^2 + e_1 (\dot{i}_{s-ref} - \dot{i}_s) \quad (13)$$

The impact of the term $e_1 (\dot{i}_{s-ref} - \dot{i}_s)$ on the global system stability will be checked at the end of the Backstepping control process. A first local control law i_{s-ref} is deduced by identification of \dot{V}_1 in (12) and (13):

$$-c_1 e_1 = C_{bus} \dot{u}_{bus-ref} - \dot{i}_{s-ref} + \dot{i}_{ts} - C_{bus} \dot{\hat{\theta}}_1 \quad (14)$$

$$i_{s-ref} = c_1 e_1 + C_{bus} \dot{u}_{bus-ref} + \dot{i}_{ts} - C_{bus} \dot{\hat{\theta}}_1 \quad (15)$$

and

$$\dot{\hat{\theta}}_1 = -C_{bus} e_1 \Gamma_1 \quad (16)$$

such that

$$-C_{bus} e_1 \Delta\theta_1 - \Delta\theta_1 \Gamma_1^{-1} \dot{\hat{\theta}}_1 = 0 \quad (17)$$

The first local control law output is reference current i_{s-ref}

(15). It is defined through a controller consisting of a control law and an update law to obtain $\hat{\theta}_1$. i_{s-ref} is an input of the next local control loop.

B. FC current loop (BS2)

From (2) and (4), a FC local control loop is required to control the currents i_{fc_ch} from the boost chopper duty cycles α_{fc_ch} (16). The unknown parameter θ_2 is introduced to represent inductor or source model inaccuracies. In real-time, α_{fc_ch} varies at the rate of the sampling frequency. α_{fc_ch} is then assumed constant by parts so that from (2) and (4) we obtain

$$\dot{i}_{fc_ch} = \alpha_{fc_ch} \left(\frac{1}{L_{fc}} \left(u_{fc} - \alpha_{fc_ch} u_{bus} - r_{fc} \frac{i_{fc_ch}}{\alpha_{fc_ch}} \right) + \theta_2 \right) \quad (18)$$

Error e_2 is defined as:

$$\begin{cases} e_2 = i_{fc_ch-ref} - i_{fc_ch} \\ \dot{e}_2 = \dot{i}_{fc_ch-ref} - \alpha_{fc_ch} \left(\frac{1}{L_{fc}} \left(u_{fc} - \alpha_{fc_ch} u_{bus} - r_{fc} \frac{i_{fc_ch}}{\alpha_{fc_ch}} \right) + \theta_2 \right) \end{cases} \quad (19)$$

To develop the current controller, *clf* V_2 is defined as:

$$\begin{cases} V_2 = \frac{1}{2} \frac{L_{fc}}{\alpha_{fc_ch}} e_2^2 + \frac{1}{2} \alpha_{fc_ch} \Delta\theta_2 \Gamma_2^{-1} \Delta\theta_2 \\ \dot{V}_2 = \frac{L_{fc}}{\alpha_{fc_ch}} e_2 \dot{e}_2 - \alpha_{fc_ch} \Delta\theta_2 \Gamma_2^{-1} \dot{\hat{\theta}}_2 \end{cases} \quad (20)$$

where Γ_2 is a positive constant, and

$$\Delta\theta_2 = \theta_2 - \hat{\theta}_2 \quad (21)$$

To impose the stability condition $\dot{V}_2 \leq 0$ with constant $c_2 \geq 0$

$$\dot{V}_2 = -c_2 e_2^2 / \alpha_{fc_ch} \quad (22)$$

(20) and (22) are compared using (19), (20) and (21) and the assumption of slow variations of θ_2 , to develop the control law for α_{fc_ch} and the associated uncertainty estimator:

$$\frac{-c_2 e_2}{\alpha_{fc_ch}} = L_{fc} \frac{\dot{i}_{fc_ch-ref}}{\alpha_{fc_ch}} + r_{fc} \left(\frac{i_{fc_ch-ref}}{\alpha_{fc_ch}} - \frac{e_2}{\alpha_{fc_ch}} \right) \quad (23)$$

$$\begin{aligned} & -u_{fc} + \alpha_{fc_ch} u_{bus} - L_{fc} \dot{\hat{\theta}}_2 \\ \alpha_{fc_ch} = & 1/u_{bus} \left(-L_{fc} \frac{\dot{i}_{fc_ch-ref}}{\alpha_{fc_ch}} - r_{fc} \left(\frac{i_{fc_ch-ref}}{\alpha_{fc_ch}} - \frac{e_2}{\alpha_{fc_ch}} \right) \right. \\ & \left. + u_{fc} - c_2 \frac{e_2}{\alpha_{fc_ch}} + L_{fc} \dot{\hat{\theta}}_2 \right) \end{aligned} \quad (24)$$

and

$$\dot{\hat{\theta}}_2 = -L_{fc} e_2 \Gamma_2 / \alpha_{fc_ch} \quad (25)$$

such that

$$-L_{fc} e_2 \Delta\theta_2 - \alpha_{fc_ch} \Delta\theta_2 \Gamma_2^{-1} \dot{\hat{\theta}}_2 = 0$$

C. SC current loop (BS3)

The SC local control law α_{sc_ch} is deduced in the same way as for the FC control loop. The unknown parameter θ_3 is added to represent other inductor or source model inaccuracies. α_{sc_ch} is assumed constant by parts:

$$\dot{i}_{sc_ch} = \alpha_{sc_ch} \left(\frac{1}{L_{sc}} \left(u_{sc} - \alpha_{sc_ch} u_{bus} - r_{sc} \frac{i_{sc_ch}}{\alpha_{sc_ch}} \right) + \theta_3 \right) \quad (26)$$

$$\alpha_{sc_ch} = 1/u_{bus} \left(-L_{sc} \frac{\dot{i}_{sc_ch-ref}}{\alpha_{sc_ch}} - r_{sc} \left(\frac{i_{sc_ch-ref}}{\alpha_{sc_ch}} - \frac{e_3}{\alpha_{sc_ch}} \right) + u_{sc} - c_3 \frac{e_3}{\alpha_{sc_ch}} + L_{sc} \hat{\theta}_3 \right) \quad (27)$$

and

$$\dot{\hat{\theta}}_3 = -L_{sc} e_3 \Gamma_3 / \alpha_{sc_ch} \quad (28)$$

where c_3 and Γ_3 are positive constants and:

$$e_3 = i_{sc_ch-ref} - i_{sc_ch} \quad (29)$$

$$\Delta \theta_3 = \theta_3 - \hat{\theta}_3 \quad (30)$$

D. Stability and controller scheme analysis

The global system stability is guaranteed if the derivative of the global *clf* V_{global} is negative (31). Replacing i_{s-ref} using (5), (7), e_2 (19) and e_3 (29) in (31) leads to (32).

$$\dot{V}_{global} = \dot{V}_1 + \dot{V}_2 + \dot{V}_3 \quad (31)$$

$$\begin{aligned} \dot{V}_{global} &= -c_1 e_1^2 - c_2 e_2^2 / \alpha_{fc_ch} - c_3 e_3^2 / \alpha_{sc_ch} + e_1 (i_{s-ref} - i_s) \\ &= - \begin{bmatrix} e_1 & e_2 & e_3 \end{bmatrix} A \begin{bmatrix} e_1 \\ e_2 \\ e_3 \end{bmatrix} \end{aligned} \quad (32)$$

with

$$A = \begin{bmatrix} c_1 & -\frac{1}{2} & -\frac{1}{2} \\ -\frac{1}{2} & c_2 / \alpha_{fc_ch} & 0 \\ -\frac{1}{2} & 0 & c_3 / \alpha_{sc_ch} \end{bmatrix} \quad (33)$$

From (33), the derivative of V_{global} is negative if the symmetrical matrix A is positive. Considering that $\alpha_{fc_sc_ch} \in [0,1]$ and using the Sylvester criterion [26], A is positive and the global system is stable if the following conditions are satisfied:

$$\begin{aligned} c_2 &> 0 \\ c_3 &> 0 \\ c_1 &> \frac{1}{16c_2} + \frac{1}{16c_3} \end{aligned} \quad (34)$$

It should be noted that the introduction of the distribution criterion k_D from (7) does not alter these conditions if k_D dynamical variations are slower than the current loop dynamics.

From (24) and (27), the tuning inputs α_{fc_ch} and α_{sc_ch} control laws can be broken down into six parts to achieve the same form as the inversion-based control scheme (equation numbers are listed on Fig. 2):

$$i_{fc-ref} = i_{fc_ch-ref} / \alpha_{fc_ch} \quad (35)$$

$$u_{fc_ch-ref} = -L_{fc} \dot{i}_{fc-ref} + L_{fc} \hat{\theta}_2 - r_{fc} \left(i_{fc-ref} - \frac{e_2}{\alpha_{fc_ch}} \right) + u_{fc} - c_2 \frac{e_2}{\alpha_{fc_ch}} \quad (36)$$

$$\alpha_{fc_ch} = u_{fc_ch-ref} / u_{bus} \quad (37)$$

$$i_{sc-ref} = i_{sc_ch-ref} / \alpha_{sc_ch} \quad (38)$$

$$u_{sc_ch-ref} = -L_{sc} \dot{i}_{sc-ref} + L_{sc} \hat{\theta}_3 - r_{sc} \left(i_{sc-ref} - \frac{e_3}{\alpha_{sc_ch}} \right) + u_{sc} - c_3 \frac{e_3}{\alpha_{sc_ch}} \quad (39)$$

$$\alpha_{sc_ch} = u_{sc_ch-ref} / u_{bus} \quad (40)$$

The control laws defined by V_{global} , (15), (36) and (39) define three controller schemes, which depend on feedback constants c_i and integral update laws $\hat{\theta}_i$ with gains Γ_i , $i=\{1,2,3\}$. These integral functions result from the disturbance estimation with the unknown parameters θ_1 , θ_2 and θ_3 . The resulting closed loop controllers on Fig. 2 take the form of Proportional Integral (PI) controllers C_{Pii} with proportional terms $k_{pi}=f(c_i)$ and integral terms $k_{ii}=f(\Gamma_i)$, $i=\{1,2,3\}$, to ensure the robustness of the system. The control schemes deduced from adaptive Backstepping control are then depending on PI controllers and parameters of the studied system. Compensation of the disturbance current i_{is} and voltages u_{fc} and u_{sc} are also used. Finally anticipation terms, the inversion of the transfer functions G_i , $i=\{1,2,3\}$, act on the reference state variables $u_{bus-ref}$, i_{fc-ref} and i_{sc-ref} using derivative terms. Equations (15), (36) and (39) are then factored as follows:

$$i_{s-ref} = G_1^{-1} u_{bus-ref} + i_{is} + e_1 C_{P11} \quad (41)$$

with $C_{P11} = k_{p1} + k_{i1} / s = c_1 + (C_{bus}^2 \Gamma_1) / s$ and $G_1^{-1} = C_{bus} s$

$$u_{fc_ch-ref} = u_{fc} - (G_2^{-1} i_{fc-ref} + e_2 C_{P12} / \alpha_{fc_ch}) \quad (42)$$

with $C_{P12} = k_{p2} + k_{i2} / s = c_2 - r_{fc} + (L_{fc}^2 \Gamma_2) / s$ and $G_2^{-1} = L_{fc} s + r_{fc}$

$$u_{sc_ch-ref} = u_{sc} - (G_3^{-1} i_{sc-ref} + e_3 C_{P13} / \alpha_{sc_ch}) \quad (43)$$

with $C_{P13} = k_{p3} + k_{i3} / s = c_3 - r_{sc} + (L_{sc}^2 \Gamma_3) / s$ and $G_3^{-1} = L_{sc} s + r_{sc}$

IV. REAL-TIME VALIDATION

A. Experimental setup

The simulation of the Backstepping control of the studied FC/SC vehicle has been carried out in [16]. Nevertheless, simulation studies are limited by modelling assumptions. Based on the traction characteristics of the Tazzari Zero battery electric vehicle [27], a reduced scale validation is proposed on an experimental platform (Fig. 4). It is composed of a 1.2 kW Ballard FC, a bank of Maxwell SC, two smoothing inductors, two choppers, and a controlled current source to emulate the traction subsystem (Fig. 1). The controlled current source is then chosen as a load drive with a ratio current reduction of 40

compared to the full-scale studied vehicle (Table 2). Voltages and currents are measured with classical LEM transducers. No additional numerical filters have been added.

B. Energy management strategy

A filtering strategy is considered for the FC/SC power distribution to avoid fast FC power dynamics, which are limited by the FC air compressor supply. This kind of strategy is often used due to its simplicity and robustness for real-time implementation [28]. The FC power must be positive with a frequency below 100 mHz to reduce stack faults and degradations [29]. The SC then provides the resulting transient power. Herein, a low-pass filter with cut-off frequency $f_c=15\text{ mHz}$ is used for the distribution parameter k_D :

$$k_D = \frac{2\pi f_c}{2\pi f_c + s} \quad (44)$$

As a consequence, k_D has slow dynamics compare to the internal current loop, which satisfies stability conditions. From k_D and (7), the low-frequency source current part is provided by the FC and the high-frequency source current part by the SC (45). In addition, the distribution criterion is augmented to include a saturation function to impose $i_{fc_ch} > 0$. This guarantees to have an exclusively positive power for the fuel cell. It may be noted that more advanced distribution strategies based on optimization methods could be proposed by changing the value of k_D [17].

$$i_{fc_ch-ref} = \text{sat} \left(\frac{2\pi f_c}{2\pi f_c + s} i_{s-ref} \right) = \begin{cases} 0 & \text{if } \frac{2\pi f_c}{2\pi f_c + s} i_{s-ref} \leq 0 \\ \frac{2\pi f_c}{2\pi f_c + s} i_{s-ref} & \text{if } \frac{2\pi f_c}{2\pi f_c + s} i_{s-ref} > 0 \end{cases} \quad (45)$$

$$i_{sc_ch-ref} = i_{s-ref} - i_{fc_ch-ref}$$

C. Results and Discussion

The developed Backstepping control scheme, the energy management strategy and the traction emulation are implemented in a dSPACE 1103 controller board using MATLAB-Simulink™. The sampling period is set to $t_{samp}=200\ \mu\text{s}$. It should be noted that the synchronized sampling naturally filters the discontinuous values of the traction system current i_{ts} . A standard driving cycle for light vehicles homologation, WLTC, for a class 2 vehicle is first considered (Fig. 5a). The controller parameters c_i and Γ_i , $i=\{1,2,3\}$, are identified based on pole placement controller tuning design [30]. The roots of the second order characteristic equation of each control loop characterize the error dynamics transients, i.e. their poles. The poles are placed according to the desired response time.

The driving cycle imposes a traction current i_{ts} in function of the emulated vehicle characteristics and control (Fig. 6a). By the use of the distribution criterion k_D , the chosen filtering strategy leads to use the SC for fast and regenerative braking power transients while the FC handles low frequencies positive powers (Fig. 6b). All the powers, currents and voltages are plotted in per-unit.



Fig. 4. Experimental platform

TABLE 2. STUDIED FC/SC VEHICLE PARAMETERS

Full-scale FC/SC EV	
Fuel Cell	55-78 V / 20 kW
Supercapacitors	54 V, 130 F
Smoothing inductors	0.25 mH / 5.5 mΩ
DC bus capacitor	80 V / 53 mF
Electric drive	15 kW
Vehicle	811 kg
FeedBack constants	$c_1 = 0.26, c_2 = c_3 = 1.6$
Adaptation gains	$\Gamma_1 = 1.6 \cdot 10^4,$ $\Gamma_2 = \Gamma_3 = 8.04 \cdot 10^8$

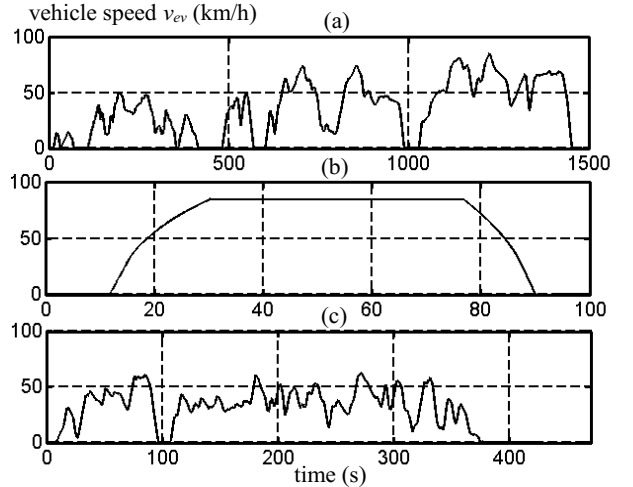


Fig. 5. Considered driving cycles
(a) WLTC of class 2, (b) acceleration test, (c) real driving cycle

The DC bus power ($P_{bus}=u_{bus} \cdot i_s$) is then compensated by both sources and reaches a maximum of $1\ pu$ in traction and a minimum of $-0.35\ pu$ in braking phase. The FC and SC voltages depend on their corresponding currents (Fig. 6c). It should be noted that the initial SC voltage u_{sc} at $t=0\ s$ is equal to $0.5\ pu$. The final voltage u_{sc} at $t=1,500\ s$ has the same value. The energy balance of the filtering strategy is zero because the electrical losses are negligible within the experimental period of $1,500\ s$.

The developed Backstepping control manages the coupling to maintain the DC bus voltage to $80\ V=1\ pu$ (Fig. 7a). The DC bus voltage variation is $\pm 5\%$. The voltage drops are negligible with respect to the electric drive supply. At all time, the FC and the SC currents are well managed because they track their references delivered by the traction requirement (Fig. 7a

b and *c*). Experimental results demonstrate that the Backstepping control of the energetic coupling is implementable in real-time conditions. As expected, the real-time conditions do not affect the stability of the controlled system due to the real-time disturbance estimation and update into the controllers. In this way, the supercapacitors can help the fuel cell to meet the requirements of the load with a guarantee of system stability in real-time.

A comparison with classical PI controllers is proposed to show the improvement in term of transient behaviour. Fig. 8 compares the experimental control performance of the DC bus voltage u_{bus} , for the PI and backstepping based controllers and three driving cycles: WLTC, an acceleration test and an urban driving cycle from an on-road test realized around the University of Lille 1 (Fig. 5). The voltage tracking performances are close. However, the PI control (red curves) shows greater voltage oscillations, particularly when the power flow dynamics are important (purple framed areas in Fig. 8). Here, the emulated system has been properly designed. The control loops also respects the system time constants because an expertise of the system has been developed during this work. It is therefore logical, and even preferable, that both Backstepping and PI controllers have similar overall performances.

V. CONCLUSION

This paper deals with a stable control for a fuel cell vehicle using supercapacitors with a Backstepping control technique for real-time implementation. EMR has been used to organize the Backstepping control scheme in a clear way for this coupled system. In this way, three Backstepping cascaded control loops, coupled by a distribution criterion, have been devised. Each Backstepping control loop has been designed to impose a local stable behavior. Moreover the global stability of the whole system has also been demonstrated. The developed Backstepping control has been validated in real-time on an experimental setup. Experimental results have shown that the supercapacitors can help the fuel cell to meet the power requirements with a guarantee of system stability for the cascaded loops. Moreover, if the same architecture is kept, the depicted method can be used for other hybrid vehicle as a fuel cell/battery vehicle without any additional consideration. As indicated in [31], the control organization of a battery / supercapacitor system could be the same. For the future, more advanced strategies could be used for the same control organization. Backstepping control laws include derivative operations that could be sensitive to large step reference variations. Additional work is required to manage saturation effects at the control law development stage.

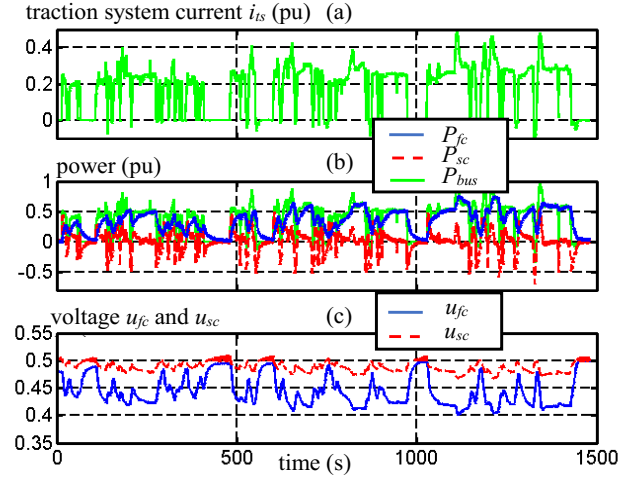


Fig. 6. Global experimental results for the WLTC driving cycle: traction current load, power distribution and fuel cell and supercapacitor voltages

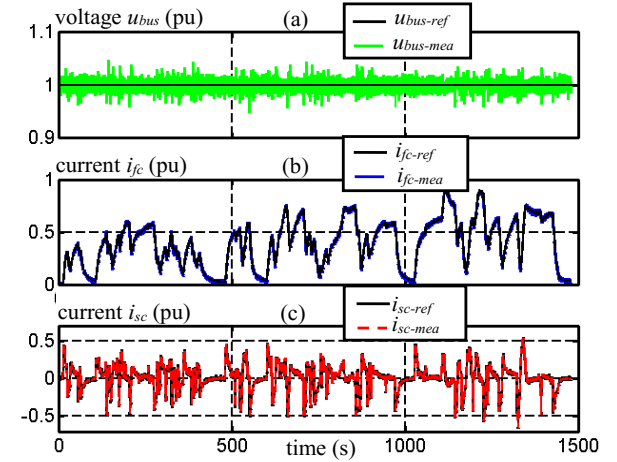


Fig. 7. State variables control for the WLTC driving cycle: DC bus voltage, fuel cell and supercapacitor currents

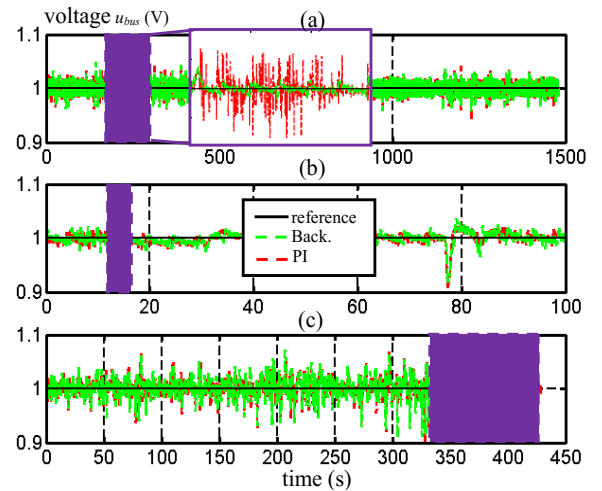
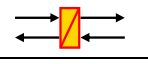
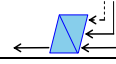
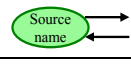
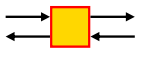
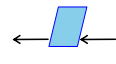

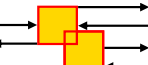
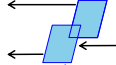



Fig. 8. DC bus voltage u_{bus} for PI and backstepping based controllers for three driving cycles. (a) WLTC of class 2, (b) acceleration test, (c) real driving cycle

REFERENCES

- [1] A. Veziroglu, and R. Macario, "Fuel cell vehicles: State of the art with economic and environmental concern", *International Journal of Hydrogen Energy*, vol. 36, no. 1, pp. 25–43, Jan. 2011.
- [2] A. Khaligh and L. Zhihao, "Battery, ultracapacitor, fuel cell, and hybrid energy storage systems for electric, hybrid electric, fuel cell, and plug-in hybrid electric vehicles: State of the art", *IEEE Trans. Veh. Technol.*, vol. 59, no. 6, pp. 2806–2814, Jul. 2010.
- [3] R. Álvarez-Fernández, F. Beltrán Cilleruelo, and I. Villar Martínez, "A new approach to battery powered electric vehicles: A hydrogen fuel-cell range extender system", *International Journal of Hydrogen Energy*, vol. 41, no. 8, pp. 4808–4819, Mar. 2016.
- [4] A. Payman, S. Pierfederici, F. Meibody-Tabar, and B. Davat, "An adapted control strategy to minimize DC-bus capacitors of a parallel fuel cell/ultracapacitor hybrid system", *IEEE Trans. Power Ele.*, vol. 26, no. 12, pp. 3843–3852, Aug. 2009.
- [5] Honda, Honda Fuel Cell Power – FCX. *Press Release*, available on the world wild web at: <http://world.honda.com/FuelCell/FuelCellVehicle-history/FCX-2002/index.html>, date accessed: March 2017.
- [6] H. Aouzellag, K. Ghedamsi, and D. Aouzellag, "Energy management and fault tolerant control strategies for fuel cell/ultra-capacitor hybrid electric vehicles to enhance autonomy, efficiency and life time of the fuel cell system", *International Journal of Hydrogen Energy*, vol. 40, no. 22, pp. 7204–7213, Jun. 2015.
- [7] H. Hemi, J. Ghouili, and A. Cheriti, "Combination of Markov chain and optimal control solved by Pontryagin's minimum principle for a fuel cell/supercapacitor vehicle", *Energy Conversion and Management*, vol. 91, pp. 387–393, Dec. 2015.
- [8] P. Thounthong, L. Piegari, S. Pierfederici, and B. Davat, "Nonlinear intelligent DC grid stabilization for fuel cell vehicle applications with a supercapacitor storage device", *International Journal of Electrical Power & Energy Systems*, vol. 64, pp. 723–733, Jan. 2015.
- [9] J. Jia, Q. Li, Y. Wang, Y. T. Cham, and M. Han, "Modeling and dynamic characteristic simulation of a proton exchange membrane fuel cell", *IEEE Trans. Ener. Conv.*, vol. 24, no. 1, pp. 283–291, Jan. 2009.
- [10] H. El Fadil, F. Giri, J.M. Guerrero, and A. Tahri, "Modeling and nonlinear control of a fuel cell/supercapacitor hybrid energy storage system for electric vehicles", *IEEE Trans. on Vehicular Technology*, vol. 63, no. 7, pp. 3011–3018, Sep. 2014.
- [11] M. Rajabzadeh, S. Mohammad Taghi Bathaee, and M. Aliakbar Golkar, "Dynamic modeling and nonlinear control of fuel cell vehicles with different hybrid power sources", *International Journal of Hydrogen Energy*, vol. 41, no. 30, pp. 3185–3198, Jan. 2016.
- [12] J. Zhou, and C. Wen, "Backstepping control", in *Control and Mechatronics*, CRC Press, pp. 20–1 – 20–22, ISBN 9781439802878, Feb. 2011.
- [13] W. Dong, J. A. Farrell, M.M. Polycarpou, and V. Djapic, "Command filtered adaptive backstepping", *IEEE Trans. Control Syst. Technol.*, vol. 20, no. 3, pp. 566–580, Mar. 2011.
- [14] O. Herizi, and S. Barkat, "Backstepping control and energy management of hybrid DC source based electric vehicle", *EFEA 2016*, Belgrade, Serbia, Sept. 2016.
- [15] C. Dépature, P. Sicard, A. Bouscayrol, W. Lhomme, and L. Boulon, "Comparison of Backstepping control and Inversion Based Control of a range extender electric vehicle", *IEEE VPPC'14*, Coimbra, Portugal, Oct. 2014. A. Bouscayrol, J.P. Hautier, and B. Lemaire-Semail, "Graphic formalisms for the control of multi-physical energetic systems: COG and EMR", *Systemic Design Methodologies for Electrical Energy Systems*, Chap. 3, Wiley-ISTE, ISBN 9781848213883, Oct. 2012.
- [16] C. Dépature, W. Lhomme, P. Sicard, A. Bouscayrol, and L. Boulon, "Backstepping control of a fuel cell/supercapacitor system for electric vehicle", *IEEE VPPC'16*, Hangzhou, China, Oct. 2016.
- [17] L. Zubieta, and R. Bonert, "Characterization of double-layer capacitors for power electronics application", *IEEE Trans. Ind. App.*, vol. 36, no. 1, pp. 199–205, Feb. 2000.
- [18] A.L. Allègre, A. Bouscayrol, and R. Trigui, "Flexible real-time control of a hybrid energy storage system for electric vehicles", *IET Electrical Systems in Transportation*, vol. 3, no. 3, pp. 79–85, Mar. 2013.
- [19] J. Solano Martínez, D. Hissel, M.C. Pera, and M. Amiet, "Practical control structure and energy management of a testbed hybrid electric vehicle", *IEEE Trans. on Vehicular Technology*, vol. 60, no. 9, pp. 4139–4152, Sep. 2011.
- [20] W. Lhomme, P. Delarue, A. Bouscayrol, P. Lemoigne, P. Barrade, A. Rufer, "Comparison of control strategies for maximizing energy in a supercapacitor storage subsystem", *EPE Journal*, vol. 19, no. 3, pp. 5–14, Sep. 2009.
- [21] C. M. Lee, S. H. Han, C. H. Zheng, and L. We-Song, "Power split of fuel cell/ultracapacitor hybrid power system by backstepping sliding mode control", *10th Int. Power & Energy Conference (IPEC)*, Ho Chi Minh City, Vietnam, Dec. 2012.
- [22] C. Kaddissi, J. P. Kenné, and M. Saad, "Indirect adaptive control of an electrohydraulic servo system based on nonlinear Backstepping", *IEEE Trans. Mechatron.*, vol. 16, no. 6, pp. 1171–1177, Dec. 2011.
- [23] W. S. Black, P. Haghi, and K. B. Ariyur, "Adaptive systems: History, techniques, problems, and perspectives", *systems*, vol. 2, pp. 606–660, 2014.
- [24] P.V. Kokotovic, "The joy of feedback: Non linear and adaptive," *IEEE Trans. Control Syst.*, vol. 12, no. 3, pp. 7–17, Jun. 1992.
- [25] H.K. Khalil, "Nonlinear systems", *New Jersey : Prentice Hall*, Chapter "Lyapunov Stability", pp. 111 – 194, ISBN 978-0130673893, 2001.
- [26] R. A. Horn, and C. R. Johnson, "Matrix Analysis", Chapter 7: Positive Definite and Semidefinite Matrice, *Cambridge University Press*, ISBN 978-0-521-83940-2, 2013.
- [27] Tazzari zero website', <http://www.tazzari-zero.com/>, accessed February 06th 2016
- [28] T. Azib, O. Bethoux, G. Remy, and C. Marchand, "Saturation management of a controlled fuel-cell/ultracapacitor Hybrid Vehicle", *IEEE Trans. on Vehicular Technology*, vol. 60, no. 9, pp. 4127–4138, Nov. 2011.
- [29] V. Liso, M. Pagh Nielsen, and S. Knudsen Koer, "Thermal modeling and temperature control of a PEM fuel cell system for forklift application", *International Journal of Hydrogen Energy*, vol. 39, pp. 8410–8420, Apr. 2014.
- [30] K. Ogata, "Design of Control Systems in State Space", in *Modern Control Engineering, Fourth Edition*, Prentice Hall, pp. 826–951, ISBN 0-13-060907-2, USA, 2002.
- [31] A. Castaings, W. Lhomme, R. Trigui, A. Bouscayrol,, "Real-time energy management strategies of a battery/supercapacitors system for Electric Vehicle under limitations", *Applied Energy*, Vol. 163, February 2016, pp.190–200

APPENDIX: EMR PICTOGRAMS

	Energy accumulation (ex. inductor)		Closed-loop control		Energy source (ex. fuel cell)
	Mono-domain converter (ex. chopper)		Open-loop control		Sensor
	Energy distribution (mono-domain)		Coupling inversion with distribution criterion		Energy management



Clément Dépature received his master's degree in Electrical Engineering from the Université Lille1 (France) in 2011. In 2011, he worked as an engineer at L2EP, in Lille. He was in charge of the development of an experimental platform dedicated to electric and hybrid vehicles and of the Tazzari Zero

monitoring.

He obtained a Ph.D in collaboration with the L2EP and the GREI (Groupe de Recherche en électronique Industrielle) of the Université du Québec à Trois-Rivières (Canada) in 2017. Since 2017, he holds a postdoctoral position at the Hydrogen Research Institute. His research activities deal with modeling, linear and non-linear control and energy management for fuel cell, hybrid and electric vehicles.



Walter Lhomme (M'16) received the M.S. degree in 2004, and the Ph.D. degree in 2007, both in electrical engineering, from the University Lille 1, Sciences and Technologies, Villeneuve d'Ascq, France, specializing on graphical description tools and methods for modeling and control of

electrical systems.

He worked as hybrid electric vehicle engineer within the Department Controls, Hybrid Vehicle Technologies Team at AVL Powertrain UK Ltd., England, for 1 year. Since September 2008 he has been engaged as Associate Professor at the Laboratory of Electrical Engineering and Power Electronics of Lille (L2EP), University Lille 1. Since 2008, he is the responsible of the experimental platform "electricity & Vehicle" of the L2EP at the University Lille 1. His research activities deal with the graphical descriptions, modelling, control, energy management and hardware-in-the-loop simulations applied in hybrid and electric vehicles field.



Pierre Sicard (S'84–M'85) received the M.S. degree in industrial electronics from the University du Québec à Trois-Rivières, Trois-Rivières QC, Canada, in 1990, and the Ph.D. degree in electrical engineering from Rensselaer Polytechnic Institute, Troy NY, in 1993.

He joined the Université du Québec à Trois-Rivières in 1992 where he has been Professor in Electrical and Computer Engineering since 2001. He held the Hydro-Québec Research Chair on Power and Electrical Energy from 1999 to 2003 and he was Director of the Research Group on Industrial Electronics from 2004 to 2011. His current research interests include modeling, controller and observer design for nonlinear systems, including motor drive control, control of electromechanical systems, multi-drive systems, load sharing control problems, control in power electronics, adaptive control, and artificial intelligence.



Alain Bouscayrol (M'02) received a Ph.D. degree in Electrical Engineering from the Institut National Polytechnique de Toulouse, France, in 1995.

From 1996 to 2005, he was Associate Professor at University Lille1, France, where he has been a Professor since 2005.

Since 2004, he has managed the national network on Energy Management of Hybrid Electric Vehicles France. He has initiated the Energetic Macroscopic Representation (EMR) in 2000 for the description and the control of energetic systems. His research interests at the L2EP include graphical descriptions for control of electric drives, wind energy conversion systems, railway traction systems, hybrid electric vehicles and hardware-in-the-loop simulation.



Loïc Boulon (M'10, SM'16) received the master degree in electrical and automatic control engineering from the University of Lille (France), in 2006. Then, he obtained a PhD in electrical engineering from University of Franche-Comté (France). Since 2010, he is a professor at Université du

Québec à Trois-Rivières (Canada) and he works at the Hydrogen Research Institute (Full Professor since 2016). His work deals with modeling, control and energy management of multiphysics systems. His research interests include hybrid electric vehicles, energy and power sources (especially battery in cold weather operation), and fuel cell systems. He has published more than 100 scientific papers in peer-reviewed international journals and international conferences.

In 2015, Loïc Boulon was general chair of the IEEE-Vehicular Power and Propulsion Conference in Montréal (QC, Canada). Prof. Loïc Boulon is VP-Motor Vehicles of the IEEE Vehicular Technology Society and he is the holder of the Canada Research Chair in Energy Sources for the Vehicles of the future.